Physiologically Based Pharmacokinetic Models of 2′,3′-Dideoxyinosine

Hyo-Jeong K. Kang,[1] M. Guillaume Wientjes,[1,2,3] and Jessie L.-S. Au[1,2,3,4]

Received October 21, 1996; accepted December 16, 1996

Purpose. The goal of this study was to develop physiologically based pharmacokinetic (PBPK) models for 2′,3′-dideoxyinosine (ddI) in rats when the drug was administered alone (ddI model) and with pentamidine (ddI + pentamidine model), and to use these models to evaluate the effect of our previously reported pentamidine-ddI interaction on tissue ddI exposure in humans.

Methods. The PBPK models consisted of pharmacologically relevant tissues (blood, brain, gut, spleen, pancreas, liver, kidney, lymph nodes, muscle) and used the assumptions of perfusion-rate limited tissue distribution and linear tissue binding of ddI. The required physiologic model parameters were obtained from the literature, whereas the pharmacokinetic parameters and the tissue-to-plasma partition coefficients were calculated using plasma and tissue data.

Results. The ddI model in rats yielded model-predicted concentration-time profiles that were in close agreement with the experimentally determined profiles after an intravenous ddI dose (5% deviation in plasma and 20% deviation in tissues). The ddI + pentamidine model incorporated the pentamidine-induced increases of ddI partition in pancreas and muscle. The two PBPK models were scaled-up to humans using human physiologic and pharmacokinetic parameters. A comparison of the model-predicted plasma concentration-time profiles with the observed profiles in AIDS patients who often received ddI with pentamidine showed that the ddI model underestimated the terminal half-life ($t_{1/2,\beta}$) by 39% whereas the ddI + pentamidine model yielded identical $t_{1/2,\beta}$ and area-under-the-curve as the observed values (<1% deviation). Simulations of ddI concentration-time profiles in human tissues using the two models showed that pancreas and lymph nodes received about 2- to 30-fold higher ddI concentration than spleen and brain, and that coadministration of pentamidine increased the AUC of ddI in the pancreas by 20%.

Conclusions. Data of the present study indicate that the plasma ddI concentration-time profile in patients were better described by the ddI + pentamidine model than by the ddI model, suggesting that the pentamidine-induced changes in tissue distribution of ddI observed in rats may also occur in humans.

KEY WORDS: ddI; physiologic pharmacokinetic model; tissue concentration; pentamidine; rat; human.

INTRODUCTION

2′,3′-Dideoxyinosine (ddI) is used to treat patients infected by human immunodeficiency virus (HIV), and patients with acquired immunodeficiency syndrome (AIDS). Several organs are important targets for this drug. These include: (a) brain because of the prevalence of AIDS dementia complex and its association with HIV infection in the central nervous system (1–2); (b) lymph nodes because they have been shown to harbor most HIV in early stages of the disease and are the sites where active viral replication occurs during the clinical latency period (3); (c) other lymphoid tissues which are targeted by the virus; and (d) pancreas because of potentially lethal pancreatitis (4). Tissue pharmacokinetic data of ddI, while they are important to elucidate the therapeutic efficacy of ddI treatment, are not readily available in humans because of limitations on tissue accessibility.

We and others have studied the plasma pharmacokinetics of ddI in animals and humans, using compartmental analysis where the plasma and rapidly perfused tissues are lumped into a central compartment and the slowly equilibrating tissues are lumped into one or more peripheral compartments (5–8). The major limitations of a compartmental body pharmacokinetic model are the lack of physiological relevance and the inability to distinguish the fate of the drug in different tissues, and hence the inability to predict the time course of drug concentration in target tissues. In contrast, a physiologically based pharmacokinetic (PBPK) model, which takes into account physiologically relevant tissue arrangement, volume and perfusion rate as well as tissue binding and metabolism, can be used to depict the tissue concentration-time profiles and used for interspecies scale-up because of the similarity of anatomy, physiology, biochemistry, and cellular structure in mammalian species. The present report describes the development of two PBPK models for ddI in rats; i.e. when ddI was administered alone (ddI model) and in combination with pentamidine (ddI + pentamidine model), and the preliminary application of these models for interspecies scale-up to humans. We previously showed that pentamidine increased the accumulation of ddI in pancreas and muscle (9).

MATERIALS AND METHODS

Chemicals and Reagents

ddI was obtained from the National Cancer Institute (Bethesda, MD). Reagent grade chemicals and high pressure liquid chromatographic (HPLC) grade solvents were purchased from Sigma Chemical Co. (St. Louis, MO) and Fisher Scientific (Cincinnati, OH).

[1] College of Pharmacy, 500 West 12th Avenue, The Ohio State University, Columbus, Ohio 43210.

[2] Division of Urology, College of Medicine, The Ohio State University, Columbus, Ohio 43210.

[3] Comprehensive Cancer Center, The Ohio State University, Columbus, Ohio 43210.

[4] To whom correspondence should be addressed. (e-mail: au.l@osu.edu)

ABBREVIATIONS: ddI, 2′,3′-dideoxyinosine; HIV, human immunodeficiency virus; AIDS, acquired immunodeficiency syndrome; PBPK, physiologically based pharmacokinetic model; HPLC, high-pressure liquid chromatography; R_{tissue}, tissue-to-plasma partition coefficient; $CL_{intrinsic}$, intrinsic clearance; V_{tissue}, tissue volume; Q_{tissue}, tissue perfusion rate; f_p, free fraction in plasma; C_p, plasma concentration; C_t, tissue concentration; C_o, drug concentration in efferent plasma; CL_{TB}, total body clearance; CL_{renal}, renal clearance; $CL_{nonrenal}$, nonrenal clearance; E_{tissue}, tissue extraction ratio; MRT, mean residence time; $t_{1/2,\beta}$, terminal half-life; AUC, area under the concentration-time profile; Vd_{ss}, volume of distribution at steady state; C_{tissue}/C_{plasma}, tissue-to-plasma concentration ratio.

0724-8741/97/0300-0337$12.50/0

Model Development—Overview

Development and verification of the PBPK model was performed in the following five steps. (A) Outline and arrange pharmacologically important tissues in an anatomically correct order. (B) Define the process of drug distribution from blood to organs. (C) Establish the mass balance equations for each organ and obtain the required physiological and pharmacokinetic parameters. (D) Substitute the model parameters into the differential mass balance equations for plasma and tissues to generate computer simulations of plasma and tissue concentration-time profiles. (E) Verify the model by comparing the model-predicted plasma and tissue concentration-time profiles with the observed profiles.

Interspecies scale-up to humans was performed in the following three steps. (A) Substitute the physiological and pharmacokinetic parameters for rats with parameters for humans into the model, while retaining the tissue-to-plasma partition parameters established from the rat data. (B) Use the model to generate a plasma concentration-time profile in humans, which was compared with the observed profile to evaluate the model validity. (C) Use the validated PBPK model to generate the concentration-time profiles in human tissues.

Model Selection

Figure 1 is the schematic representation of the PBPK model for ddI. The model includes pharmacologically important tissues (brain, spleen, lymph nodes, pancreas), and the eliminating organs (gut, liver, kidney) (8–10). In addition, muscle was included because of the significant drug distribution to this tissue and its large volume.

The assumptions for the PBPK model are: (a) intercompartmental transport occurs via blood flow; (b) instantaneous equilibrium between tissue and blood within the tissue; (c) equal drug concentration in effluent blood and blood within the tissue; (d) same unbound drug concentrations in plasma and tissues; and (e) only unbound drug molecules are eliminated. Plasma concentrations were used instead of blood concentrations because of the equal distribution of ddI in blood cells and plasma (8). Total drug concentration in plasma was taken as the free drug concentration ($f_p = 1$), because of the insignificant plasma protein binding of ddI of between 2–5% at a concentration range of 0.5 to 50 μg/ml in rat and human plasma (11–12).

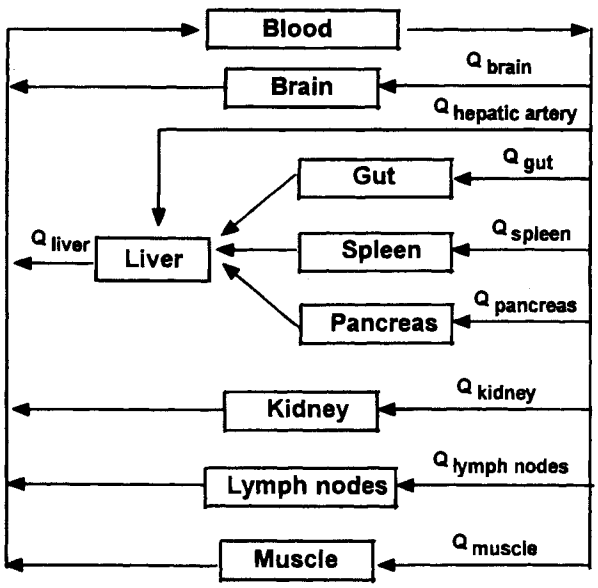

Fig. 1. Schematic diagram of the physiologic pharmacokinetic model for ddI.

ddI is a relatively small compound (MW 236) with a pKa of 9 (13). ddI is a substrate of the nucleoside transporter and also transported via nonfacilitated diffusion in RBC (14). However, ddI is not a substrate of nucleoside and nucleobase transporters in lymphocytes, macrophages, and bone marrow cells (15). It is not known which transport process is responsible for ddI transport in different tissues. However, the rapid equilibrium of ddI between plasma and tissues with no saturable uptake over a wide concentration range of 0.2 to 300 μg/ml (16) suggests that ddI distribution from blood to tissues is perfusion-limited rather than transport-limited.

Figure 2 shows the relationship between tissue concentrations and plasma concentrations, constructed using our previously reported plasma and tissue concentration-time data of ddI after an intravenous bolus injection (16) and the infusion data from the present study. The plots show linear relationships with slopes of about 1 for all tissues, for concentrations spanning over 3 orders of magnitude. This indicates the absence of saturable binding, and suggests linear tissue binding (17).

Differential Mass Balance Equations

Differential mass balance equations were written for individual tissues according to standard methods (18). Equation 1

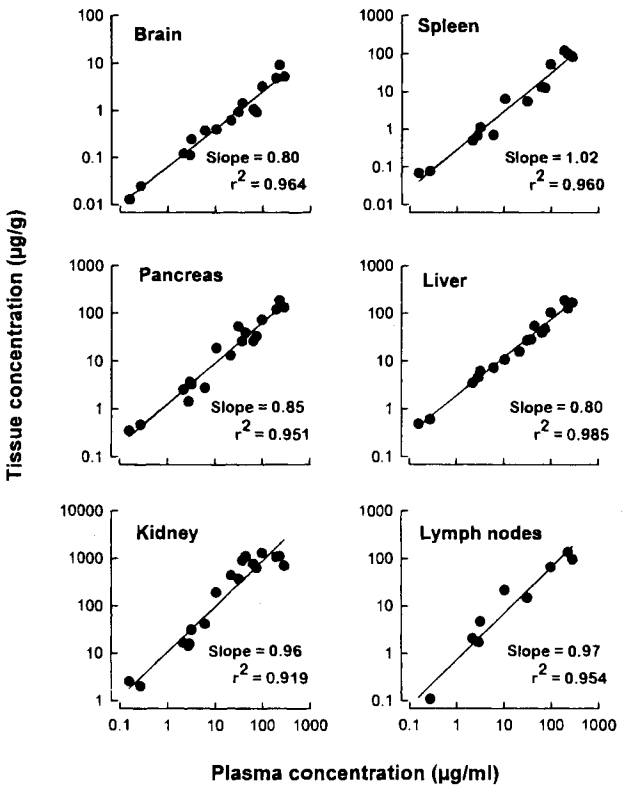

Fig. 2. Tissue concentrations versus plasma concentrations (log-log plots). Rats were given an intravenous bolus injection of 100 mg/kg or infusion of 2 mg/min/kg of ddI. Slopes and correlation coefficients (r^2) of the regressed lines are indicated.

shows the mass balance equation for blood which is the input compartment, equation 2 for a non-eliminating organ (brain, pancreas, lymph nodes, muscle), equation 3 for an eliminating organ (gut, spleen, kidney), and equation 4 for liver which is anatomically unique because it receives blood supplies from gut, spleen, and pancreas:
for blood,

$$V_p \cdot \frac{dC_p}{dt} = Dose + \left(\Sigma Q_{tissue} \cdot \frac{C_{tissue}}{R_{tissue}}\right) - (\Sigma Q_{tissue}) \cdot C_p \quad (1)$$

for a non-eliminating organ,

$$V_{tissue} \cdot \frac{dC_{tissue}}{dt} = Q_{tissue} \cdot C_p - Q_{tissue} \cdot \frac{C_{tissue}}{R_{tissue}} \quad (2)$$

for an eliminating organ,

$$V_{tissue} \cdot \frac{dC_{tissue}}{dt} = Q_{tissue} \cdot C_p - (Q_{tissue} + CL_{intrinsic}) \cdot \frac{C_{tissue}}{R_{tissue}} \quad (3)$$

for liver,

$$V_{liver} \cdot \frac{dC_{liver}}{dt} = (Q_{liver} - Q_{gut} - Q_{spleen} - Q_{pancreas}) \cdot C_p + Q_{gut} \cdot \frac{C_{gut}}{R_{gut}} + Q_{spleen} \cdot \frac{C_{spleen}}{R_{spleen}} + Q_{pancreas} \cdot \frac{C_{pancreas}}{R_{pancreas}} - (Q_{liver} + CL_{intrinsic,\ liver}) \cdot \frac{C_{liver}}{R_{liver}} \quad (4)$$

where V_{tissue} is tissue volume, C_{tissue} is total drug concentration in tissue, Q_{tissue} is tissue perfusion rate, $CL_{intrinsic}$ is intrinsic clearance, C_p is plasma concentration, and R_{tissue} is tissue-to-plasma partition coefficient. The term C_{tissue}/R_{tissue} represents drug concentration in efferent plasma (C_o) since R_{tissue} is defined as C_{tissue}/C_o (18).

Parameter Selection and Calculation

The required physiologic parameters are tissue volumes and tissue perfusion rates, and were obtained from the literature (19–21). The required pharmacokinetic parameters, i.e. $CL_{intrinsic}$ and R_{tissue} were either experimentally determined or calculated from previously published data.

The $CL_{intrinsic}$ for liver, gut, spleen, and kidney were derived from the in vivo plasma pharmacokinetic data, i.e. renal (CL_{renal}) and nonrenal ($CL_{nonrenal}$) clearances. Elimination of ddI in rats and humans is mainly by metabolism and renal excretion (6,10,22). In rats, liver is the major metabolizing organ for ddI, while the small intestine and spleen account for about 20% of hepatic metabolism (10,16). The following assumptions were used: (a) linear drug elimination, based on the linear elimination of ddI over plasma concentrations of 0.2 to 500 μg/ml in rats (8,23), which were comparable to the concentration range in the present study; (b) the relative magnitude of $CL_{intrinsic}$ of each tissue is proportional to the size and the in vitro metabolic activity per g of tissue; (c) identical metabolic activity per g of tissue for spleen and liver, based on the nearly identical degradation half-life of ddI in spleen and liver homogenates (10,16); (d) elimination in gut occurs only in small intestine (10); (e) same relative metabolic activity in human tissues as in rat tissues; and (f) $CL_{nonrenal}$ is due to metabolism in liver, spleen and small intestine.

The CL_{renal} and $CL_{nonrenal}$ accounted for 17% and 83% of the total body clearance (CL_{TB}) in rats (8), and 51% and 49% of the CL_{TB} in AIDS patients (6). $CL_{intrinsic}$ in kidney was calculated using equation 5 (18). E_{tissue} is the tissue extraction ratio and is represented by equation 6. $E_{nonrenal}$, which represents the extraction in the three metabolizing organs that are linked by their blood supplies, i.e. liver, spleen, and small intestines, is described in equation 7. Equations 6 and 7 were solved simultaneously using a numerical method.

$$CL_{intrinsic,\ kidney} = \frac{CL_{renal}}{1 - E_{kidney}} \quad (5)$$

$$E_{tissue} = \frac{CL_{tissue}}{Q_{tissue}} = \frac{CL_{intrinsic,\ tissue}}{Q_{tissue} + CL_{intrinsic,\ tissue}} \quad (6)$$

$$E_{nonrenal} = E_{liver} \cdot \left(1 - \frac{Q_{spleen} + Q_{small\ intestine}}{Q_{liver}}\right) + [(1 - E_{spleen}) \cdot E_{liver} + E_{spleen}] \cdot \frac{Q_{spleen}}{Q_{liver}} + [(1 - E_{small\ intestine}) \cdot E_{liver} + E_{small\ intestine}] \cdot \frac{Q_{small\ intestine}}{Q_{liver}} \quad (7)$$

Animal Protocol for Determination of Tissue and Plasma Concentrations

Tissue and plasma data were obtained after intravenous bolus injection and slow infusion of ddI in female Fisher rats. The animal experiments were in compliance with the Guide for the Care and Use of Laboratory Animals, NIH publication 86-23. The concentration-time profiles in brain, spleen, liver, kidney, lymph node, and pancreas for an intravenous bolus injection of ddI alone (n = 16 rats) and after a continuous infusion of ddI alone (n = 3) and ddI plus pentamidine (n = 3) were obtained from previous studies (9,16). An additional study used two rats to obtain the concentration-time profiles in muscle and gut, after an infusion. The protocols were as described previously (16). In brief, rats (Charles River, Wilmington, MA), 5–6 months of age and weighing 220 ± 20 g, were anesthetized with ether and catheters were implanted in the tail vein or the right jugular vein. ddI was infused through the tail vein catheter for 2 to 3 hr (200 to 240 mg/kg) or administered as a bolus dose (100 mg/kg) through the jugular vein catheter. In the combination therapy study, ddI (200 mg/kg) and pentamidine (10 mg/kg) were given simultaneously for 3 hr. Rats were anesthetized with ether 3–5 min before the predetermined times. Tissue removal and processing, extraction and analysis of plasma and tissue samples were as described previously (16).

Determination of R_{tissue} in Rats

R_{tissue} can be determined under in vitro or in vivo conditions. There is no general agreement on the best method for

determining R_{tissue} (24–25), but the in vivo method is commonly used. We determined R_{tissue} during steady state following intravenous infusion or after a bolus intravenous dose. For determination of R_{tissue} from bolus injection data, we used the hybrid model which is relatively insensitive to data fluctuation and requires less data. The hybrid model has been used to estimate the transport and binding parameters in tissues (17,26). In the hybrid model, the C_p term in the mass balance equations (equations 2, 3, 4) was substituted with a time-dependent input function, which is the plasma concentration-time data expressed as a mathematical function. For ddI, we used a biexponential function, $C_p = A \cdot e^{-\alpha \cdot t} + B \cdot e^{-\beta \cdot t}$. The resulting equation was fitted to the observed concentration-time profile to solve for the best-fit $R_{tissue,hybrid}$ for individual tissues. For the infusion method, R_{tissue} equals the tissue-to-plasma concentration ratio at steady state ($R_{tissue,ss}$) (24). For gut and muscle where we did not have the profiles after an intravenous bolus dose, we used $R_{tissue,ss}$ from the infusion study because the $R_{tissue,hybrid}$ and $R_{tissue,ss}$ for other tissues were comparable. For eliminating organs, the $R_{tissue,ss}$ and $R_{tissue,hybrid}$ values for liver, spleen, gut and kidney were adjusted for elimination in the tissue by equation 8 (24). The R_{tissue} values were substituted into mass balance equations (equations 1 through 4) to simultaneously simulate concentration-time profiles in plasma and tissues (i.e. global model simulation) (17).

$$R_{tissue} = R_{tissue,hybrid} \cdot \left(1 + \frac{CL_{intrinsic}}{Q_{tissue}}\right) \quad \text{or}$$

$$R_{tissue} = R_{tissue,ss} \cdot \left(1 + \frac{CL_{intrinsic}}{Q_{tissue}}\right) \quad (8)$$

The R_{tissue} values determined for one animal species may apply to other species, provided that drug distribution follows principles of thermodynamic partitioning with relatively minor interspecies variation and that the two species have similar Vd_{ss} values of the drug (18). Because the Vd_{ss} of ddI in several species are in comparable ranges, i.e. 0.77 l/kg for humans (6), 0.9–1.8 l/kg for monkeys (7,27), 0.6–0.8 l/kg for rats (8), and 0.7–0.9 l/kg for dogs (5), the $R_{tissue,hybrid}$ and $R_{tissue,ss}$ values determined in rats, after adjusted for the $CL_{intrinsic}$ in humans using equation 8, were used for simulation in humans.

Alteration by Pentamidine

We previously reported that in rats, pentamidine coadministration altered the ddI distribution to pancreas and muscle but not spleen, liver, and kidney (9). Pentamidine is often coadministered with ddI to AIDS patients (28–29). Replacement of $R_{pancreas}$ and R_{muscle} in the ddI PBPK model with $R_{pancreas}$ and R_{muscle} obtained during ddI and pentamidine treatments resulted in the second PBPK model, i.e. ddI + pentamidine model.

Comparison of Volume of Distribution at Steady State (Vd_{ss})

To evaluate the reasonableness of the R_{tissue} values established from tissue distribution studies, the apparent volume of distribution at steady state ($Vd_{ss,model}$) calculated from R_{tissue} using equation 9, was compared with the volume estimated from the plasma pharmacokinetic data ($Vd_{ss,plasma}$) using equation 10 (20).

$$Vd_{ss,tissue} = V_{tissue} \cdot R_{tissue} \cdot (1 - E_{tissue}) \quad \text{and}$$

$$Vd_{ss,model} = \sum Vd_{ss,tissue} \quad (9)$$

$$Vd_{ss,plasma} = CL_{TB} \cdot MRT \quad (10)$$

where V_{tissue} is anatomical tissue volume and MRT is mean residence time. E_{tissue} is tissue extraction ratio and was set to zero for non-eliminating organs.

Computer Simulations and Data Analysis

Computer fitting and simulations were done using PCNONLIN (SCI Software, Lexington, KY). A weight function of 1/concentration was used for fitting of the hybrid models. The area under the concentration-time curve (AUC), CL_{TB}, mean residence time (MRT), and terminal half-life ($t_{1/2,\beta}$) were calculated according to standard procedures (30).

RESULTS

Model Parameter Selection

Table 1 summarizes the physiologic and pharmacokinetic parameters for the PBPK models. To determine if the literature values were appropriate, wet tissue weights were determined for brain, spleen, liver and kidney in 17 rats. The weights for individual tissues were comparable to the reported tissue volume: the average difference in weight and volume was 25%, with brain giving the least difference (13%) and liver giving the highest difference (33%). The blood flow rates to regional lymph nodes are not available and could not be easily determined experimentally. As an estimation of the blood flow to

Table 1. Physiological and Pharmacokinetic Parameters[a]

	Tissue volume (ml)		Blood flow (ml/min)		$CL_{intrinsic}$ (ml/min)[d]	
Tissue	Rat	Human	Rat	Human	Rat	Human
Blood	12.0	5,400	NA[b]	NA[b]	0.0[e]	0.0[e]
Brain	1.5	1,450	1.33	700	0.0[e]	0.0[e]
Gut	8.8	1,650	7.52	1,100	0.81	42.3
Spleen	0.53	192	0.63	77	0.35	35.4
Pancreas	1.15	84	0.51	134	0.0[e]	0.0[e]
Liver	9.06	1,690	11.8	1,650	6.01	312
Kidney	2.0	310	9.23	1,100	1.06	524
Lymph nodes	0.8	280	0.087[c]	8.26[c]	0.0[e]	0.0[e]
Muscle	112	35,000	7.5	750	0.0[e]	0.0[e]

Note: The physiological parameters are for a 220 g rat and 70 kg man.

[a] Tissue volume and blood flow parameters were obtained from the literature (19–21).

[b] NA: not applicable.

[c] Calculated as the product of [V_{tissue}] and [the average of the perfusion rate per ml tissue for skin (0.15 ml/min/ml for rats and 0.038 ml/min/ml for humans) and muscle (0.067 ml/min/ml for rats and 0.021 ml/min/ml for humans)].

[d] Values calculated from reported data in literature using equation 5 through 7 as described in Methods (6,8,16).

[e] Assumed no metabolism in these tissues.

lymph nodes, which have low capillary density, we used the average value of blood flow rat per ml tissue to skin and muscle. Using these parameters, the ddI PBPK model was established.

Verification of the ddI PBPK Model

The ddI PBPK model predicted concentration-time profiles in rat plasma and tissues that were comparable to the biexponential profiles observed experimentally (Figure 3). The predicted profiles in brain, spleen, pancreas, liver and kidney are similar to the plasma profile, showing biexponential decays with a short distribution phase and elimination phase. This similarity suggests a rapid equilibrium between plasma and these tissues. In contrast, the predicted profiles in lymph nodes and muscle showed an early uprising phase followed by a decline. The differences between the profiles in lymph nodes and muscle with the other tissues suggest that lymph nodes and muscle are slowly equilibrating tissues. On average, the model-predicted $t_{1/2,\beta}$ and AUC deviated from the observed values by 5% and 14% in plasma and by 22% and 24% (range of −40 to +23% for $t_{1/2,\beta}$ and −10 to −36% for AUC) in tissues. The CL_{TB} calculated from the model-predicted plasma concentration-time profile was 24.2 ml/min/kg which was comparable with the observed value of 20.9 ml/min/kg. The agreement between predicted and observed values indicated the validity of the model.

ddI + Pentamidine PBPK Model

The ddI + pentamidine model incorporated the pentamidine-induced changes in ddI distribution to pancreas and muscle, as follows. An intravenous infusion of pentamidine, which produced a steady state concentration of 350 ng/ml, increases the $C_{pancreas}$:C_{plasma} and C_{muscle}:C_{plasma} ratios of ddI in rats by 150% and 540%, respectively (9). In AIDS patients, a 600 mg inhalation dose of pentamidine produced peak and trough plasma concentrations of 9 and 89 ng/ml, respectively (31), and accordingly an average concentration of 49 ng/ml. This concentration is 13% of the steady state concentrations in rats (9). Assuming that the extent of increases in $R_{pancreas}$ and R_{muscle} by pentamidine is linearly related to pentamidine concentration, we estimated that pentamidine coadministration in man would increase $R_{pancreas}$ and R_{muscle} by 19% (i.e. 13% × 150%) and 70% (i.e. 13% × 540%), respectively. The ddI + pentamidine model in man used the pentamidine-modified $R_{pancreas}$ and R_{muscle} values.

Application of PBPK Models to Humans

Figure 4 shows the predicted plasma concentration-time profiles in humans by the ddI and ddI + pentamidine PBPK models. The ddI model yielded a profile that superimposed the observed profile up to 120 min and an AUC that was nearly

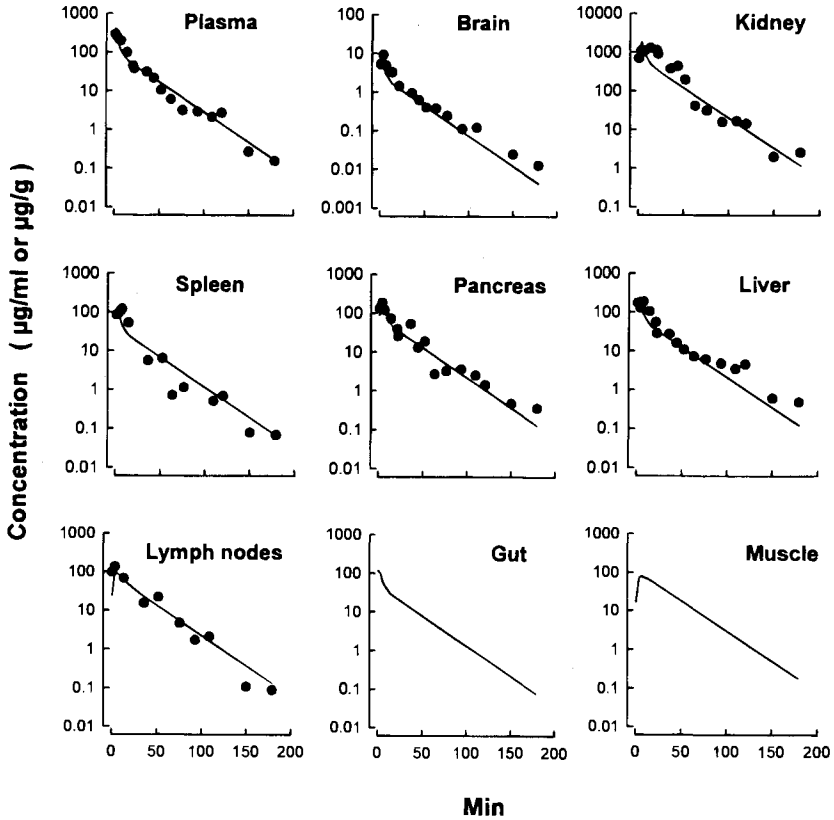

Fig. 3. Predicted and observed concentrations of ddI in plasma and tissues after an intravenous bolus injection of ddI of 100 mg/kg. The observed data were taken from a previous study (16). Each data point represents an individual rat. Solid lines represent simulated profiles using the ddI PBPK model. Note that profiles for gut and muscle after a bolus dose were not experimentally determined. The profiles in these two tissues were predicted using the R_{tissue} obtained from the infusion study.

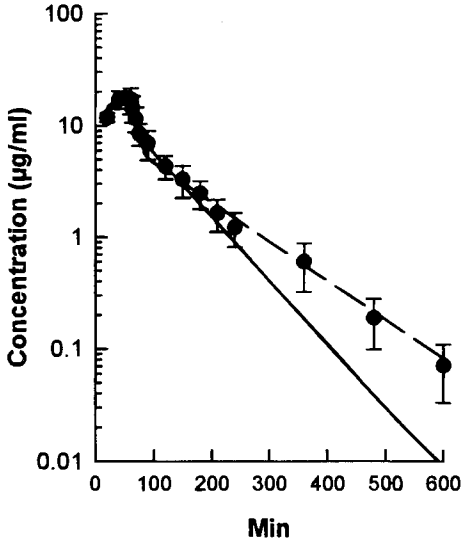

Fig. 4. Comparison of model-predicted plasma concentration-time profiles in humans with observed profiles in AIDS patients. Data from patients (●) were obtained from a published study (6) in which patients were given an 1 hr intravenous infusion of 16.5 mg/kg ddI. Simulated profiles using the ddI model (solid line) and the ddI + pentamidine model (dashed line).

identical to the observed value (0.6% deviation), but underestimated the concentration from 150 to 600 min and accordingly underestimated the $t_{1/2,\beta}$ (39% lower than the observed value). The ddI + pentamidine PBPK model yielded a profile that better described the observed profile than the ddI model, resulted in nearly identical $t_{1/2,\beta}$ and AUC (deviated from the observed values by <1%), suggesting the ddI + pentamidine model as the more appropriate model.

Figure 5 shows the simulated concentration-time profiles of ddI in human tissues using the ddI + pentamidine PBPK model. Simulated data using the ddI + pentamidine model

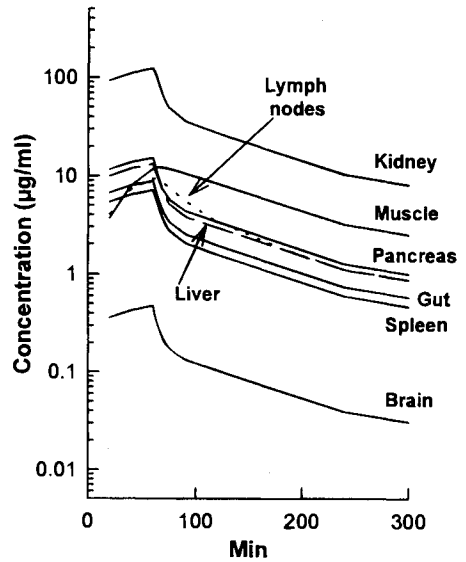

Fig. 5. Simulated tissue concentration-time profiles in patients using the ddI + pentamidine model. Note that profiles for liver and lymph nodes merged after 180 min.

yielded a 18% and 69% greater drug accumulation in pancreas and muscle, respectively, than the data using the ddI model (data not shown).

Volume of Distribution at Steady State

Table 2 summarizes the $Vd_{ss,model}$ of ddI in rat and human tissues. In rats, the $Vd_{ss,model}$ calculated using R_{tissue} when ddI was administered alone was 0.53 l/kg, which was about 10% higher than the $Vd_{ss,plasma}$ of 0.48 l/kg calculated from the plasma data. In humans, the $Vd_{ss,model}$ calculated using the pentamidine-modified R_{tissue} was 5% smaller than the $Vd_{ss,plasma}$, i.e. 0.73 vs 0.77 l/kg. The comparable values of $Vd_{ss,model}$ and $Vd_{ss,plasma}$ in rats and humans indicate the reasonableness of the R_{tissue} used in the PBPK models. In both species, distribution to muscle, due to the combined effect of its high tissue volume and moderate R_{tissue}, accounted for 67 to 80% of $Vd_{ss,model}$. The well perfused organs, i.e., liver, kidney, and blood, together accounted for 17 to 28% of $Vd_{ss,model}$ due to their intermediate tissue volumes and high (kidney) and moderate (liver and blood) R_{tissue}.

DISCUSSION

The goal of the present study was to develop PBPK models for ddI, either administered alone or in combination with pentamidine. The results in rats show that the ddI PBPK model adequately described the ddI concentration-time profiles in plasma and tissues, and yielded Vd_{ss} that was comparable to the value determined using independent methods. These data indicate the validity of the ddI PBPK model. The second model, i.e. ddI + pentamidine model, was developed to account for the pentamidine-induced changes in drug distribution to pancreas and muscle. When these two models were applied for interspecies scale-up to humans, the ddI + pentamidine model but not the ddI model yielded a plasma ddI concentration-time profile that superimposed the profile observed in AIDS patients who often received ddI in combination with pentamidine (6). This supports the validity of the ddI + pentamidine PBPK model in humans, and suggests that the pentamidine-induced increases in drug accumulation in pancreas and muscle that were observed in rats might have also occurred in humans. There are several examples of increased Vd_{ss} and/or tissue concentration by the addition of a second drug, i.e. verapamil by lidocaine in dogs (32), adriamycin by verapamil in humans (33), 5-fluorouracil by bromodeoxyuridine in dogs (34), cefotaxime by mezlocillin in humans (35), and thiopental by halothane in rats (36). Further verification of this hypothesis requires tissue distribution data in humans, which are unlikely to be available. Another approach would be to expand the studies to include other animal species to validate the interspecies scale-up application of the PBPK models.

It should be noted that AIDS patients often receive multiple medications (prescribed and non-prescribed). There may be other drug interactions that account for the differences in the model-predicted and the observed plasma concentration-time profiles in humans. Other interspecies differences such as tissue distribution (e.g. tissue binding and transport) and metabolism (e.g. metabolism in tissues other than liver, spleen, and small

Table 2. R_{tissue} and $Vd_{ss,model}$

Tissue	Rat			Man		
	$R_{tissue} \cdot (1 - E_{tissue})$	$Vd_{ss,tissue}$[a] (ml)	% of total $Vd_{ss,model}$	$R_{tissue} \cdot (1 - E_{tissue})$	$Vd_{ss,tissue}$[a] (l)	% of total $Vd_{ss,model}$
Blood	1.00	12.0	10.3	1.00	5.40	10.6
Brain	0.026	0.039	0.034	0.026	0.038	0.074
Gut	0.51	4.46	3.84	0.51	0.84	1.64
Spleen	0.393	0.21	0.18	0.393	0.075	0.15
Pancreas	0.71	0.81	0.70	0.84[e]	0.070	0.14
Liver	0.76	6.90	5.95	0.76	1.29	2.52
Kidney	6.82	13.6	11.8	6.82	2.11	4.13
Lymph nodes	0.61	0.49	0.42	0.61	0.17	0.34
Muscle	0.69	77.5	66.8	1.18[e]	41.2	80.5
$Vd_{ss,model}$[b]	NA[c]	116[d]	100	NA[c]	51.2[d]	100

Note: R_{tissue} was determined under in vivo conditions after a continuous intravenous infusion to steady state or after a bolus intravenous injection. Data analysis in rats used the ddI PBPK model, whereas data analysis in humans used the ddI + pentamidine model.

[a] Calculated using equation 9.

[b] Equals sum of $Vd_{ss,tissue}$ of individual tissues in the model.

[c] NA: not applicable.

[d] $Vd_{ss,model}$ on a kg basis, calculated as (total $Vd_{ss,model}$) ÷ (body weight) (0.22 kg for rats and 70 kg for humans), was 0.53 l/kg for rats and 0.73 l/kg in humans. In comparison, the $Vd_{ss,plasma}$ calculated using equation 10 and data from the literature (6,16) were 0.48 l/kg for rats and 0.77 l/kg for humans.

[e] $R_{pancreas}$ and R_{muscle} in humans were 119% and 170% of the values in rats, respectively (see Results).

intestine) also can not be ruled out. Nonetheless, data of the present study provide the first approximation of ddI tissue pharmacokinetics in AIDS patients.

The simulated ddI concentration-time profiles in humans using the ddI and ddI + pentamidine PBPK models show that pancreas and lymph nodes received about 2- to 30-fold higher ddI concentration than spleen and brain, and that coadministration of pentamidine altered ddI accumulation in the pancreas. Lymphoid tissues and brain are the target organs for the desired therapeutic effects, whereas the pancreas is the target organ for its major toxicity. An extrapolation of these data indicates that the therapeutic efficacy of ddI can be enhanced by increasing its distribution to brain and spleen, and by decreasing its distribution to pancreas. A population pharmacokinetic analysis in AIDS patients suggests that concomitant use of pentamidine was one of the predictors of pancreatitis (37). Because pentamidine alone produces pancreatic toxicity (38–39), the enhanced toxicity may be related to cumulative effect of the two drugs. On the other hand, the pentamidine-induced increase of ddI accumulation in pancreas, albeit relatively minor, represents an alternative/additional mechanism of the potentiated pancreatic toxicity in patients receiving both ddI and pentamidine that warrants further investigation.

ACKNOWLEDGMENTS

This work was supported in part by research grants RO1 AI28757 and RO1 AI29133 from the National Institute of Allergy and Infectious Diseases, and a Research Career Development Award (KO4 CA01497) to J. L.-S. Au from the National Cancer Institute. The authors thank Dr. David W. Hobson for his suggestions and assistance on the PBPK modeling, and Dr. Catherine A. Knupp for providing the plasma concentration-time data in AIDS patients.

REFERENCES

1. S. Koenig, H. E. Gendelman, J. M. Orestein, M. C. Dal Canto, G. H. Pezeshkpour, M. Yungbluth, F. Janotta, F. Aksamit, M. A. Martin, and A. S. Fauci. *Science* **223**:1089–1093 (1986).
2. G. M. Shaw, M. E. Harper, B. H. Hahn, L. G. Epstein, D. C. Gajdusek, R. W. Price, B. A. Navia, C. K. Petto, C. J. O'Hara, J. E. Groopman, E.-S. Cho, J. M. Oleske, F. Wong-Staal, and R. C. Gallo. *Science* **227**:177–181 (1985).
3. G. Pantaleo, G. Graziosi, J. F. Demarest, L. Butini, M. Montroni, C. H. Fox, J. M. Orenstein, D. P. Kotler, and A. S. Fauci. *Nature* **362**:355–358 (1993).
4. K. M. Butlar, D. Venzon, N. Henry, R. N. Husson, B. Mueller, F. M. Balis, F. Jacobson, L. L. Lewis, and P. A. Pizzo. *Pediatrics* **91**:747–751 (1993).
5. S. Kaul, C. A. Knupp, K. A. Dandekar, K. A. Pittman, and R. H. Barbhaiya. *Antimicrob. Agents Chemother.* **35**:610–614 (1991).
6. C. A. Knupp, W. C. Shyu, R. Dolin, F. T. Valentine, C. Mclaren, R. R. Martin, K. A. Pittman, and R. H. Barbhaiya. *Clin. Pharmacol. Ther.* **49**:523–535 (1991).
7. M. Qian, T. S. Finco, A. R. Swagler, and J. M. Gallo. *Antimicrob. Agents Chemother.* **35**:1247–1249 (1991).
8. M. G. Wientjes, E. Mukherji, and J. L.-S. Au. *Pharm. Res.* **9**:1070–1975 (1992).
9. T.-K. Yeh, H.-J. K. Kang, M. G. Wientjes, and J. L.-S. Au. *Pharm. Res.* **13**:626–630 (1996).
10. S. L. Bramer, J. L.-S. Au, and M. G. Wientjes. *J. Pharmacol. Exp. Ther.* **265**:731–738 (1993).
11. G. Ray and E. Murrill. *Anal. Lett.* **20**:1815–1838 (1987).
12. B. D. Anderson, B. L. Hoesterey, D. C. Baker, and R. E. Galinsky. *J. Pharmacol. Exp. Ther.* **253**:113–118 (1990).
13. B. D. Anderson, M. B. Wygant, T.-X. Xiang, W. A. Waugh, and V. J. Stella. *Int. J. Pharm.* **45**:27–37 (1988).
14. B. A. Domin, W. B. Mahony, and T. P. Zimmerman. *Biochem. Pharmacol.* **46**:725–729 (1993).
15. T. C. K. Chan, L. Shaffer, R. Redmond, and K. L. Pennington. *Biochem. Pharmacol.* **46**:273–278 (1993).
16. H.-J. K. Kang, M. G. Wientjes, and J. L.-S. Au. *Biochem. Pharmacol.* **48**:2109–2116 (1994).
17. F. G. King and R. L. Dedrick. *J. Pharmacokinet. Biopharm.* **9**:519–534 (1981).

18. M. Gibaldi and D. Perrier. *Pharmacokinetics*. 2nd Ed. Marcel Dekker, New York (1982).
19. D. H. Ringler and L. Dabich. In H. J. Baker, J. R. Lindsey, and S. H. Weisbroth (eds.), *The laboratory rat*. Vol I, Academic Press, New York, 1979, p 113.
20. A. Bernareggi and M. Rowland. *J. Pharmacokinet. Biopharm.* **19**:21–50 (1991).
21. B. Davies and T. Morris. *Pharm. Res.* **10**:1093–1095 (1993).
22. L. K. Tay, E. A. Papp, and J. Timoszik. *Biopharm. Drug Dispos.* **12**:185–197 (1991).
23. G. F. Ray, W. P. Mason, and M. Z. Badr. *Drug Metab. Dispos.* **18**:654–658 (1990).
24. H.-S. G. Chen and J. F. Gross. *J. Pharmacokinet. Biopharm.* **7**:117–125 (1979).
25. J. M. Gallo, F. C. Lam, and D. G. Perrier. *J. Pharmacokinet. Biopharm.* **15**:271–280 (1987).
26. R. J. Lutz, R. L. Dedrick, J. A. Straw, M. M. Hart, P. Klubes, and D. S. Zaharko. *J. Pharmacokinet. Biopharm.* **3**:77–97 (1975).
27. R. J. Ravasco, J. D. Unadkat, C.-C. Tsai, and C. Nosbisch. *J. Acquir. Immune Defic. Syndr.* **5**:1016–1018 (1992).
28. F. T. Valentine, M. Seidlin, H. Hochster, and M. Laverty. *Rev. Infect. Dis.* **12**:S534–539 (1990).
29. K. J. Connolly, J. D. Allan, H. Fitch, L. Jackson-Pope, C. McLaren, R. Canetta, and J. E. Groopman. *Am. J. Med.* **91**:471–475 (1991).
30. M. Rowland and T. N. Tozer. *Clinical Pharmacokinetics. Concepts and Applications*. Lea and Febiger, Philadelphia (1980).
31. J. A. Golden, M. H., Katz, D. N. Chernoff, S. M. Duncan, and J. E. Conte, Jr. *Chest* **104**:743–750 (1993).
32. J. E. Chelly, D. C. Hill, D. R. Abernethy, A. Dlewati, M.-F. Doursout, and R. G. Merin. *J. Pharmacol. Exp. Ther.* **243**:211–216 (1987).
33. D. J. Kerr, J. Graham, J. Cummings, J. G. Morrison, G. G. Thompson, M. J. Brodie, and S. B. Kaye. *Cancer Chemother. Pharmacol.* **18**:239–242 (1986).
34. D. E. Smith, D. E. Brenner, C. A. Knutsen, S. J. Deremer, P. A. Terrio, N. J. Johnson, P. L. Stetson, and W. D. Ensminger. *Drug Metab. Dispos.* **21**:277–283 (1993).
35. L. C. Rodondi, J. F. Flaherty, P. Schoenfeld, S. L. Barriere, and J. G. Gambertoglio. *Clin. Pharmacol. Ther.* **45**:527–534 (1989).
36. U. Büch, P. Altmayer, J. C. Isenberg, and H. P. Büch. *Arzneimittel-Forschung*. **41**:363–366 (1991).
37. T. H. Grasela, C. A. Walawander, M. Beltangady, C. A. Knupp, R. R. Martin, L. M. Dunkle, R. H. Barbhaiya, K. A. Pittman, R. Dolin, F. T. Valentine, and H. A. Liebman. *J. Infect. Dis.* **169**:1250–1255 (1994).
38. T. E. Herchline, J. F. Plouffe, and M. F. Para. *J. Infect.* **22**:41–44 (1991).
39. U. Balslev and T. L. Nielsen. *Dan. Med. Bull.* **39**:366–368 (1992).